A&A 439, 85–91 (2005)
DOI: 10.1051/0004-6361:20041958

Astronomy & Astrophysics

ISO observations and models of galaxies with hidden broad line regions⋆

A. Efstathiou[1] and R. Siebenmorgen[2]

[1] School of Computer Science and Engineering, Cyprus College, 6 Diogenes Street, Engomi, 1516 Nicosia, Cyprus
e-mail: efstathi@cycollege.ac.cy
[2] European Southern Observatory, Karl-Schwarzschildstr. 2, 85748 Garching b. München, Germany

Received 6 September 2004 / Accepted 31 March 2005

Abstract. We present *ISO* mid-infrared spectrophotometry and far-infrared photometry of galaxies with Hidden Broad Line Regions (HBLR). We also present radiative transfer models of their spectral energy distributions which enable us to separate the contributions from the dusty disc of the AGN and the dusty starbursts. We find that the combination of tapered discs (discs whose thickness increases with distance from the central source in the inner part but stays constant in the outer part) and starbursts provide good fits to the data. The tapered discs dominate in the mid-infrared part of the spectrum and the starbursts in the far-infrared. After correcting the AGN luminosity for anisotropic emission we find that the ratio of the AGN luminosity to the starburst luminosity, $L_{\rm AGN}/L_{\rm sb}$, ranges from about unity for IRAS 14454-4343 to about 13 for IRAS 01475-0740. Our results suggest that the warm IRAS colours of HBLR are due to the relatively high $L_{\rm AGN}/L_{\rm sb}$. Our fits are consistent with the unified model and the idea that the infrared emission of AGN is dominated by a dusty disc in the mid-infrared and starbursts in the far-infrared.

Key words. galaxies: active – infrared: galaxies – radiative transfer

1. Introduction

Since the discovery of broad lines in the polarized flux of the prototypical Seyfert 2 galaxy NGC 1068 by Antonucci & Miller (1985) much effort has been directed towards the study of this phenomenon in large samples of narrow-lined AGN (Miller & Goodrich 1990; Young et al. 1996a,b; Heisler et al. 1997; Tran 2001, 2003; Lumsden et al. 2001). The main aim was to test the unified model of active galaxies according to which many of the differences between narrow-lined and broad-lined AGN can be understood as arising from the presence of an obscuring torus viewed from different directions (Antonucci 1993).

The presence of a geometrically and optically thick dusty torus implies that a large fraction of the optical and ultraviolet radiation emitted by the central engine of the AGN is absorbed by dust and re-radiated anisotropically in the infrared (Efstathiou & Rowan-Robinson 1990, 1995; Pier & Krolik 1992; Granato & Danese 1994). Detailed radiative transfer calculations show that the predicted infrared spectrum of a dusty torus is sensitive to a number of parameters including the inclination. Deep absorption features at around 10 μm due to silicate dust are predicted for edge-on views of the torus. For face-on views a variety of spectra are predicted ranging from emission/absorption features at 10 μm to completely featureless spectra.

The spectral energy distributions (SEDs) predicted by most radiative transfer models of dusty discs and tori presented to date are generally narrower than the observed infrared SEDs. This is not necessarily a limitation of the models. NGC 1068 has in fact been known for some time to be a composite object (e.g. Telesco et al. 1984) where the Seyfert nucleus is surrounded by a 3 kpc diameter ring of star formation. The AGN dominates in the mid-infrared part of the spectrum (Rieke & Low 1975) and the starburst dominates in the far-infrared.

Rowan-Robinson & Crawford (1989) showed that a three component model (cirrus, starburst and AGN) could explain observations of IRAS galaxies. Genzel et al. (1998) argued on the basis of ISO spectroscopy that about half of the ultraluminous infrared galaxies harbour simultaneously an AGN and starburst activity. ISO spectroscopy (see also Roche et al. 1991) also showed the prevalence of mid-infrared emission features due to PAHs in AGN (Clavel et al. 2000). These features are believed to be emitted by the starburst in these systems as the radiation field is too hard for the PAH molecules to survive in the dusty torus (Roche et al. 1991; Siebenmorgen et al. 2004a).

The coexistence of dusty AGN and nuclear starbursts and the low spatial resolution of current infrared observations

⋆ Based on observations with ISO (Kessler et al. 1996), an ESA project with instruments funded by ESA Member States (especially the PI countries: France, Germany, the Netherlands and the UK) with the participation of ISAS and NASA.

require a composite starburst/AGN torus model to explain the observed SEDs. In recent years there has been considerable progress in attempts to model the SEDs emitted by starburst galaxies (Rowan-Robinson & Efstathiou 1993; Krügel & Siebenmorgen 1994; Silva et al. 1998; Efstathiou et al. 2000; Siebenmorgen et al. 2001) and axi-symmetric dust distributions in AGN (Pier & Krolik 1992; Granato & Danese 1994; Efstathiou & Rowan-Robinson 1995). These models have been successfully compared to the SEDs of a number of infrared galaxies.

The results from the different polarimetric surveys show that not all narrow-lined AGN show broad lines in polarized flux. Galaxies known to have HBLR generally show warmer infrared colours compared to galaxies without HBLR. The first interpretation of this result was that the occurrence of the phenomenon requires a special viewing geometry (Heisler et al. 1997). Later Alexander (2001), Lumsden et al. (2001) and Tran (2001, 2003) argued against this model. The cold colours of galaxies without HBLR were instead mainly attributed to the dominance of the host galaxy. Galaxies without HBLR have in general weaker AGN. This is consistent with the composite starburst/AGN torus model. Tran went a step further and argued that narrow-lined objects without HBLR do not have a broad line region at all and therefore the unified model does not apply to all AGN.

In this paper we report *Infrared Space Observatory (ISO)* mid-infrared spectrophotometric and far-IR photometric observations of two galaxies (IRAS 14454-4343 and 3C 321) that show HBLR. We use radiative transfer models to separate the contributions from starbursts and AGN to the SEDs of these two galaxies. We also model IRAS 01475-0740 for which we extracted spectrophotometric data from the *ISO* archive. The data presented here allow us to carry out the most stringent test to date to the composite starburst/AGN torus model for the infrared emission of AGN. We assume a flat Universe with $\Lambda = 0.73$ and $H_0 = 71\ \mathrm{km\,s^{-1}}$ Mpc.

2. Observations

Mid infrared spectrophotometric imaging of IRAS 14454−4343 and 3C 321 were performed on 03-Sep.-1997 using the ISOCAM circular variable filter (CVF, Cesarsky et al. 1996). The ISO archive number (TDT) of the observations are 65 800 208 for 3C 321 and 65 800 106 for IRAS 14454−4343, respectively. The observations cover a total field of $96'' \times 96''$. For each CVF step between 16.3 μm down to 6.4 μm about 30 exposures of 2.1 s integration time using the $3''$ lens were read out.

The ISOCAM data were reduced with the ISOCAM Interactive Analysis (CIA, Ott et al. 1997). We used the default data reduction steps of CIA: dark current subtraction, initial removal of cosmic ray hits (glitches), detector transient fitting, exposure coaddition and flat fielding.

The dark current depends on the orbital position of the ISO space-craft and the temperature of the ISOCAM detector. The applied correction is based on a model described by Roman & Ott (1999). The deglitching is done by following the temporal signal variation of a pixel using a multi-resolution wavelet transform algorithm (Starck et al. 1997). The response of the detector pixels strongly depends on the previous observations and there are long term hysteresis effects for each detector element after changes of the photon flux level. The detector flux transient fitting method for ISOCAM data was developed by Coulais & Abergel (2000). After application of the default deglitcher some residuals of cosmic ray impacts were still visible in the data. Therefore after the detector flux transient correction we applied a second cosmic ray rejection method which is basically a multi-sigma clipping of the temporal signal (Ott et al. 2000). To determine the source spectrum, we perform a multi–aperture photometry on each image of the different CVF steps. For all apertures centered on the brightest pixel of the source we determine the background as the mean flux derived in a 4 pixel wide annulus which is put 2 pixels away from the greatest aperture. In this way, we obtain aperture fluxes that flatten with increasing aperture radius and approach an asymptotic value. The same procedure is repeated on a theoretical and normalised point source image calculated for the central wavelength of each CVF image (Okumura 1998). This provides a correction factor of beam effects of the multi–aperture analysis. In order to derive the statistical uncertainty of the flux, we perform the same procedure on the rms image and quadratically add the rms of the background estimate. The so far reduced flux must be converted into astronomical units (mJy) by multiplication with the standard conversion factor (as given in the calibration files: CCGLWCVF1 and CCGLWCVF2 provided within CIA; see ISOCAM Handbook, Blommaert et al. 2001).

Table 1. ISOPHT photometry of IRAS 14454-4343 and 3C 321.

Name	$S_{65\ \mu m}$/Jy	$S_{90\ \mu m}$/Jy	$S_{170\ \mu m}$/Jy
IRAS 14454-4343	4.5 ± 0.3	–	2.3 ± 0.35
3C 321	–	0.78 ± 0.23	0.4 ± 0.12

Both targets were also observed with the PHT instrument at 170 μm in mini-raster mode. The TDT of the observations was 61801012 for IRAS 14454-4343 and 60201514 for 3C 321. IRAS 14454-4343 was also observed at 65 μm (TDT 61801013) and 3C 321 at 90 μm (60201515).

For the ISOPHT data standard PIA version 9 data reduction was used. The "actual" FCS responsivity, and not the default average one, was used. The photometry was derived from the small maps assuming unresolved point sources. There was no indication for a significant extended resolved flux contribution in the maps. The results of the ISOPHT data reduction are given in Table 1.

3. Radiative transfer models

3.1. Starburst models

Efstathiou et al. (2000; hereafter ERS00) developed a starburst model that includes stellar population synthesis (Bruzual & Charlot 1993), a simple model for the evolution of giant molecular clouds and detailed radiative transfer that includes the effect of transiently heated particles/PAHs. The models make

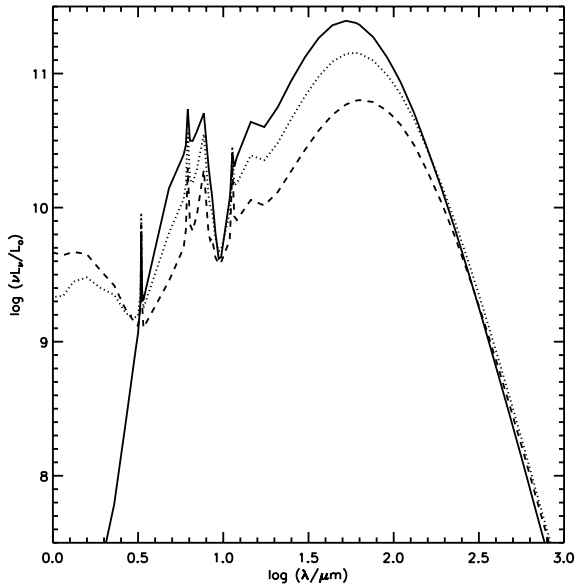

Fig. 1. Spectral energy distributions of Efstathiou et al. starbursts in which the star formation rate decays exponentially with time (time constant 30 Myr). The SED is shown for three different starburst ages: 10 Myr (solid), 40 Myr (dotted) and 70 Myr (dashed). The models assume a molecular cloud mass $M_{\rm GMC}$ of $2\times10^7\ M_\odot$, a star formation efficiency η of 0.25 and an average molecular cloud density $n_{\rm av}$ of 600 cm^{-3}. The initial star formation rate is assumed to be 100 $M_\odot$ yr^{-1}.

predictions about the emitted spectrum of starburst galaxies from the UV to the submillimeter as a function of the star formation history of the starburst and its age. Some illustrative results are given in Fig. 1. The effect of age on the SED is to make it progressively cooler with the interesting prediction that the submillimeter luminosity becomes almost independent of starburst age. Note also that the absorption feature at 10 μm gets shallower with age. The models assume that the dust to gas ratio does not evolve with age.

The ERS00 models were applied with considerable success to fit the SEDs of the nearby starbursts M 82 and NGC 6090. The models were also used to model the SEDs of ultraluminous (Farrah et al. 2003) and hyperluminous (Rowan-Robinson 2000; Verma et al. 2002; Farrah et al. 2002) infrared galaxies. In this study we consider models of the type described in ERS00 with a range of average molecular cloud densities ($n_{\rm av}$ = 300−1500 cm^{-3}) and molecular cloud masses ($M_{\rm GMC}$ = 10^7−10^8 $M_\odot$). The star formation efficiency η is kept fixed at 0.25. The models assume two more parameters: the time constant of the exponentially decaying star formation rate (τ = 1−30 Myr) and the age of the starburst (t = 0−72 Myr).

3.2. AGN models

Models of the infrared emission from dusty tori or discs in active galactic nuclei were presented by Pier & Krolik (1992, 1993), Granato & Danese (1994), Efstathiou & Rowan-Robinson (1995), van Bemmel & Dullemond (2003).

One of the principal constraints for these models were spectrophotometric observations of AGN at 8–13 μm (Roche et al. 1991). These observations showed moderate absorption features at 10 μm in type 2 AGN, which are attributed to silicates, but rather featureless spectra in type 1 AGN.

Pier & Krolik (1992) presented models of moderate to high optical depth tori which were approximated as cylinders of uniform density. The most optically thick of their models produced flat 8–13 μm spectra or moderate absorption features when the tori were viewed face-on but the SEDs were rather narrow. In their application of these models to NGC 1068, Pier & Krolik (1993) introduced an additional optically thin component that broadened the emission from the optically thick torus.

Granato & Danese (1994) presented models for flared discs of moderate optical depth. With a standard interstellar dust mixture such models predict emission features at 10 μm when the discs are viewed face-on (Efstathiou 1990). Granato & Danese showed that these features are suppressed if the silicates are destroyed (for example by shocks) in the inner part of the dusty disc. Grain mixtures that differ from the standard galactic one have also been discussed by Laor & Draine (1993), Maiolino et al. (2001a,b), van Bemmel & Dullemond (2003) and Galliano et al. (2003). Granato et al. (1994) presented a fit to the SED of the nucleus of NGC 1068 with a model that assumes that the dust density varies exponentially with a function of the polar angle Θ.

Efstathiou & Rowan-Robinson (1995, hereafter ERR95) considered anisotropic spheres (see also Rowan-Robinson et al. 1993), flared and tapered discs. Flared discs have a thickness that increases linearly with distance from the central source. The thickness of tapered discs also increases with distance in the inner disc but assumes a constant value in the outer disc. ERR95 concluded that the geometry that best fits the observational constraints is that of tapered discs. Efstathiou, Hough & Young (1995) proposed a model for the nucleus of NGC 1068 that involved a tapered disc and dust in the ionization cones. The presence of conical dust in NGC 1068 is supported by subarcsecond mid-infrared imaging (e.g. Cameron et al. 1993). If the conical dust is diffuse and composed of the standard interstellar mixture it will emit a strong silicate emission feature. This dust should therefore either be concentrated in clouds or be composed of large grains only. Efstathiou, Hough & Young attempted to model approximately the emission of conical dust by increasing the abundance of very large (30 μm) grains in the cones.

Rowan-Robinson (1995) presented a model for the infrared emission of PG quasars that treated an anisotropic distribution of clouds which were approximated by narrow shells. This model also produces weak silicate emission features and broad SEDs. The idea of a clumpy torus was explored in much more detail by Nenkova et al. (2002) who calculated the emission of individual clouds with the slab approximation. The latter authors also computed the emission/absorption by an ensemble of clouds in a flared disc.

The AGN models considered in this study are the tapered disc models described in ERR95 that represent one possible solution to the problem. For simplicity we do not consider conical dust in this paper. The reader is referred to ERR95 for a discussion of how the predicted SEDs depend on the assumed parameters. We consider tapered disc models in which we vary two parameters: the half-opening angle $\Theta_{\rm o}$ which we vary in

Table 2. Best fitted AGN torus parameters and derived luminosities: A is the anisotropy factor (see Sect. 4.1), i is the angle between the line of sight and the polar axis of the disc, Θ_o is the half-opening angle, L_{sb}, L_{AGN} and L_{tot} are the starburst, AGN and total 1–1000 μm luminosities respectively. Note that the emission from the AGN torus is anisotropy corrected (see Sect. 4). For the starburst models the best-fitted parameters for all objects are: time constant of the exponentially decaying star formation rate is 3×10^7 years, age is 7.2×10^7, average molecular cloud density 1500 cm^{-3} and molecular cloud mass 5×10^7 $M_\odot$.

Name	z	χ^2_{min}/df	A	i	Θ_o	$\log L_{AGN}/L_\odot$	$\log L_{sb}/L_\odot$	$\log L_{tot}/L_\odot$
IRAS 14454-4343	0.03856	1.19	1.4	58°	45°	11.40	11.37	11.69
3C 321	0.09610	1.26	7.3	73°	60°	12.30	11.40	12.35
IRAS 01475-0740	0.01766	0.85	1.7	60°	45°	10.78	9.67	10.81

the range 30°, to 60° (this is related to the angle Θ_1 defined by ERR95 by $\Theta_o = 90° - \Theta_1$) and the inclination i which covers the range 0 to $\pi/2$ (face- to edge-on tori). The SED is computed for 37 lines of sight equally spaced in i. The ratio of inner to outer disc radii r_1/r_2 is fixed at 0.05 which is the middle of the values considered by ERR95. The equatorial 1000 Å optical depth is kept fixed at 1000 and the ratio of disc height to inner radius h/r_1 is assumed to be 10 for all models. As in ERR95 the density distribution in the tapered disc is assumed to follow r^{-1}.

Galliano et al. (2003) carried out a comprehensive study of the prototypical Seyfert 2 galaxy and HBLR NGC 1068. They found that the nuclear SED can be fitted successfully with both tapered discs and flared discs whose density varies with polar angle Θ. Galliano et al. found that the size and optical thickness of the torus are reasonably well constrained by the data but the geometry of the torus is not. Good fits are obtained with models that assume that the inclination is in the range 30° to 50°. For reference, the model of Efstathiou et al. (1995) for the nucleus of NGC 1068 assumed an inclination of 45°. Because we are only considering a small set of tapered disc models in this paper, our predicted inclinations may be uncertain by 10–20°. This also introduces an uncertainty in the anisotropy corrected luminosity of the AGN (see Sect. 4.1).

4. Results of model fitting

Given the set of starburst and torus models described above we seek the combination which provides the minimum reduced χ^2. The torus emission can vary with the inclination but the starburst emission is assumed to be inclination-independent. Furthermore, we assume that there is no absorption of radiation emitted by the torus by the starburst and vice versa. This is not an important limitation if the starburst is concentrated in a circumnuclear ring as in the case of NGC 1068, although in such a case we may expect some heating of the outer parts of the torus by the starburst. If, however, a significant fraction of the radiation emitted by the AGN in directions not covered by the torus is intercepted by circumnuclear or galactic dust then our estimated starburst luminosity will be overestimated.

To be consistent with the fact that no broad lines are seen directly in these objects, we only consider models where the line of sight to the central source passes through the disc. The resulting fits are given in Fig. 2 and the best fit parameters are tabulated in Table 2. There are no other combinations of starburst and AGN torus/inclination that give a χ^2 lower than $\chi^2_{min} + 1$. The best fit models are found to be in good agreement with the broad band SEDs as well as the detailed ISO spectrophotometry in the 5–13 μm range.

4.1. IRAS 14454-4343

Polarized Broad H_α and H_β were discovered in IRAS 14454-4343 by Young et al. (1996a). A very good fit to the spectrophotometry and far-IR photometry is obtained with a model where i is 58°.

As it is clear from the plot of the spectral energy distribution of the torus for different inclinations given by ERR95, the emission from the torus is highly anisotropic. We quantify this with the anisotropy factor $A(i)$ which is defined to be

$$A(i) = \frac{2 \int_0^{\pi/2} S(i) \sin i \, \mathrm{d}i}{\pi S(i)}$$

where $S(i)$ is the bolometric emission at angle i.

For the specific model and inclination that gives the best fit to IRAS 1445-4343, A is 1.4 which implies that the AGN is about 40% more luminous than it would be if the observed emission was radiated isotropically. After this correction the AGN torus is found to be approximately as luminous as the starburst. The predicted intrinsic luminosity of IRAS 14454-4343 (4.9×10^{11} $L_\odot$) places this object in the Luminous Infrared Galaxy (LIRG) class.

The starburst age is predicted to be 72 Myr and the initial visual optical depth of the molecular clouds is predicted to be 250. The latter is a factor of five higher than the optical depth of molecular clouds in the M 82 and NGC 6090 starburst (ERS00). More details of assumed parameters and derived luminosities are given in Table 2.

4.2. 3C 321

A polarized broad component of H_α was discovered in this powerful FR II galaxy by Young et al. (1996b). The spectrophotometric data for this object are not as good as for IRAS 1445-4343 as this object is about an order of magnitude fainter in the mid-infrared. Nevertheless a clear 10 μm feature in absorption is detected. The best fit model is the most geometrically thin of the models considered i.e. the model with $\Theta_o = 60°$. The best fit i in this object is 73°. This implies a higher anisotropy factor which is found to be 7.3 in this case. After correcting for

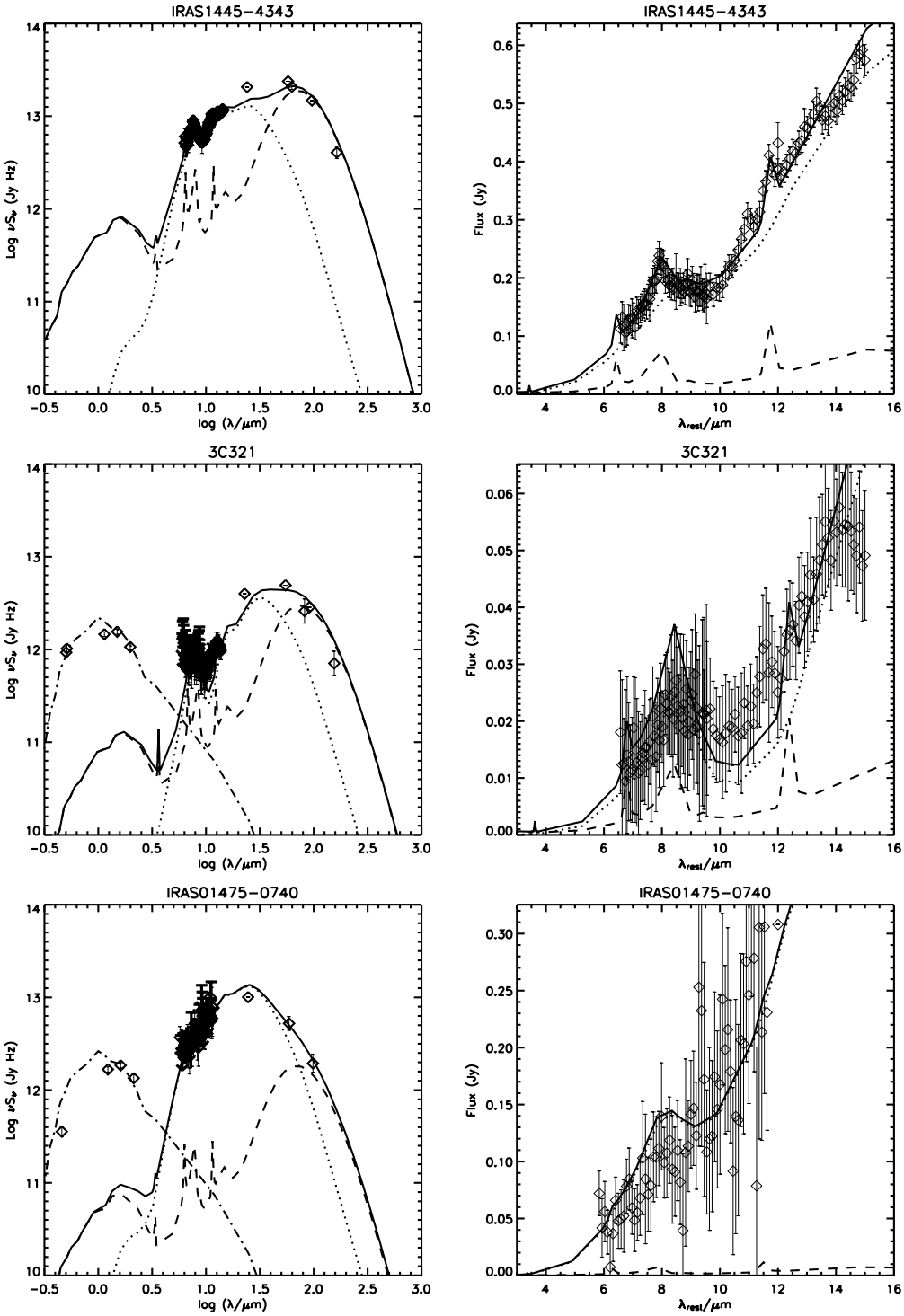

Fig. 2. Best fits to the rest frame SEDs of IRAS 14454-4343, 3C 321 and IRAS 01475-0740 with a starburst/AGN torus combination model. The total emission is plotted with a solid line whereas the individual contributions from the starburst and AGN are given by the dashed and dotted lines respectively. In the case of 3C 321 and IRAS 01475-0740 where optical/near-IR data is available, the emission by an old stellar population (12.5 Gyr) normalized to the *H* band is shown with a dash-dot line.

this effect we find that the AGN is about a factor of 8 more luminous than the starburst. The predicted intrinsic luminosity of 3C 321 ($2.2 \times 10^{12}\ L_{\odot}$) places this object in the Ultraluminous Infrared Galaxy (ULIRG) class.

The best fit starburst parameters for 3C 321 are identical to those found for IRAS 14454-4343.

4.3. IRAS 01475-0740

Polarized broad lines in this object were discovered by Tran (2001). The best fit disc model is identical to that for IRAS 1445-4343 but i is slightly higher (60°) i.e. this object is viewed more edge-on. The anisotropy correction factor is also

slightly higher (1.7). This object is the least luminous of the objects studied with a total intrinsic luminosity of $6.5 \times 10^{10}\ L_{\odot}$. Interestingly, however, it has the highest ratio of AGN to starburst luminosity (13). The fitted starburst parameters are also identical to those for IRAS 14454-4343 and 3C 321.

5. Discussion and conclusions

We presented *ISO* mid-infrared spectrophotometry and far-IR photometry for two objects (IRAS 14454-4343 and 3C 321) that show (polarized) Hidden Broad Line Regions. We also extracted from the *ISO* archive mid-IR spectrophotometry for a third object (IRAS 01475-0740) that shows the same phenomenon. We used radiative transfer models of torus and starburst emission to separate their contribution to total luminosity. We find that the combination of the tapered discs of Efstathiou & Rowan-Robinson (1995) and the starburst models of Efstathiou et al. (2000) provide good fits to the data. These results support the idea of a two-component model to explain the infrared emission of AGN. The same model has been applied to fit the SEDs of ultraluminous (Farrah et al. 2003) and hyperluminous (Morel et al. 2001; Farrah et al. 2002; Verma et al. 2002) infrared galaxies although in those studies mid-infrared spectrophotometry was not available. A similar study was carried out by Rowan-Robinson (1995) who modeled the SEDs of PG quasars with a combination of the starburst model of Rowan-Robinson & Efstathiou (1993) and a model for the AGN emission that considered an ensemble of geometricaly thin shells. Models of the type presented here were also applied to fit the SEDs of Cen A (Alexander et al. 1999) and Circinus (Ruiz et al. 2001).

Nenkova et al. (2002) presented a model that is based on the idea that the dust in AGN is concentrated in clouds. They found that if the dust is contained in 5–10 clouds (each with a visual optical depth greater than 60) along radial rays through the torus they can produce SEDs extending to the far-infrared. The broadest of the predicted SEDs shows a silicate feature in emission for type I objects. More recently, Dullemond & van Bemmel (2005) presented models of clumpy tori around active galactic nuclei and compared them with equivalent smooth tori. They found that the 10 μm emission feature of the clumpy models, when seen almost face-on, is not appreciably reduced compared to the equivalent smooth models.

Kuraszkiewicz et al. (2003) presented flared disc models for three X-ray selected active galaxies. The models reproduce the whole infrared SED without the need for a starburst component. The models presented by Kuraszkiewicz et al. show strong silicate features in emission. The latter authors note that these features would be eliminated if the torus were clumpy but as discussed above this may not necessarily be the case.

Siebenmorgen et al. (2004b) presented radiative transfer models for 3CR radio galaxies detected by ISOCAM. Although the models of Siebenmorgen et al. are spherically symmetric, they take into account for the first time the destruction of small grains and PAHs by the radiation field of the central engine of the AGN. Their models show that when the dust is at large distances from the central engine (several kpc) the SED peaks in the far-IR and strong PAH features are predicted. When the dust is close to the central engine, a situation that approximates a nuclear torus, the SEDs shift to shorter wavelengths and do not show strong PAH bands.

It would be interesting to see if the models considered in this paper and those discussed above can successfully model the detailed SEDs of AGN that will soon become available with the *Spitzer Space Telescope*.

The results from the various spectropolarimetric surveys carried out to date show that not all narrow-lined AGN contain HBLR. Heisler et al. (1997) pointed out that galaxies that harbour HBLR tend to have warm mid- to far-infrared colours ($F_{60}/F_{25} \leq 4$). To interpret this result they proposed a model according to which the orientation of the dusty torus is the main factor that determines the visibility of polarized broad lines. Heisler et al. suggested that the reason for this is that scattering takes place very close to the nucleus. In their model non-HBLRs are those narrow-lined AGN which are viewed at high inclination and therefore the scattered (and hence polarized) radiation is also blocked by the torus. In a subsequent paper Lumsden et al. (2001) presented results from a spectropolarimetric survey of a complete far-infrared selected sample of Seyfert 2 galaxies. This study confirmed the findings of Heisler et al. that galaxies with HBLR tend to have warm mid- to far-infrared colours. However, Lumsden et al. presented evidence showing that the warmth of the infrared emission is not solely due to inclination. They found instead that the main determining factor is the relative luminosity of the AGN and the host galaxy as proposed first by Alexander (2001). HBLRs are found in objects where the AGN dominates the infrared luminosity. Lumsden et al. also found that HBLRs have less obscuration than non-HBLRs of the same luminosity suggesting, that orientation may also be important if obscuration arises in a torus.

Recently Lumsden et al. (2004) presented results from a spectropolarimetric survey of a sample of Compton-thin Seyfert 2 galaxies. They found that the detection of HBLR in this sample is considerably higher than in Seyfert 2 galaxies as a whole. They also found HBLR in galaxies with cool mid- to far-infrared colours ($F_{60}/F_{25} > 4$). These observations argue against the idea proposed by Tran (2003) that there are two populations of Seyfert 2s, those with a broad line region and those without one.

The available evidence therefore suggests that the occurrence of the HBLR phenomenon requires a strong AGN relative to the host galaxy and possibly lower obscuration which may imply a dependence on inclination. The method applied in this paper allows a determination of both the ratio of AGN to starburst luminosities and the inclination. So a similar analysis on a larger sample of Seyfert 2s preferably with data provided by new space telescopes, such as the *Spitzer Space Telescope*, promises to be useful for understanding the HBLR phenomenon.

The tendency of galaxies with HBLR to show both warm mid- to far-infrared colours and evidence for strong AGN relative to the host galaxy (as measured by the [OIII] 5007 Å to H_{β} ratio) supports the idea of the two-component model for the infrared emission of AGN. Galaxies with warm colours are

objects with a strong AGN whose emission peaks in the mid-infrared and therefore boosts the 25 μm flux.

As it is evident from Fig. 2, even in objects in which the AGN dominates the bolometric luminosity, the starburst dominates at wavelengths longer than 60–100 μm. By contrast the rest-frame mid-infrared emission is dominated by the AGN torus. If we assume that the same model applies to the high redshift Universe, this result justifies the use of submillimeter and millimeter fluxes to derive star-formation rates for high redshift objects found in blank field surveys (e.g. Hughes et al. 1998; Scott et al. 2002) or pointed observations of high redshift objects (e.g. Priddey & McMahon 2001).

Acknowledgements. We are grateful to the anonymous referee for useful comments and suggestions. This work was partly carried out while AE was supported by the UK Particle Physics and Astronomy Research Council (PPARC). AE also acknowledges support by Cyprus College through a faculty grant. We are grateful to Martin Haas for making available to us the results of his reduction of the far-IR data of 3C 321 and IRAS 14454-4343. This work has made use of the NASA Extragalactic Database (NED).
Based on observations with *ISO*, an ESA project with instruments funded by ESA Member States (especially the PI countries: France, Germany, the Netherlands and the United Kingdom) with the participation of ISAS and NASA. CIA is a joint development by the ESA Astrophysics Division and the ISOCAM Consortium. The ISOCAM Consortium is led by the ISOCAM PI, C. Cesarsky. PIA is a joint development by the ESA Astrophysics Division and the ISO-PHT Consortium.

References

Alexander, D. M. 2001, MNRAS, 320, L15
Alexander, D. M., Efstathiou, A., Hough, J. H., et al. 1999, MNRAS, 310, 78
Antonucci, R. 1993, ARA&A, 31, 473
Antonucci, R. J., & Miller, J. S. 1985, ApJ, 297, 621
Blommaert, J., et al. 2001, ISO Handbook Volume III (CAM), SAI-99-057/Dc, http://www.iso.vilspa.esa.es
Bruzual, A. G., & Charlot, S. 1993, ApJ, 405, 538
Cameron, M., Storey, J. W. V., Rotaciuc, V., et al. 1993, ApJ, 419, 136
Cesarsky, C. J., Abergel, A., Agnese, P., et al. 1996, A&A, 315, L32
Clavel, J., Schulz, B., Altieri, B., et al. 2000, A&A, 357, 839
Coulais, A., & Abergel, A. 2000, A&AS, 141, 533
Dullemond, C. P., & van Bemmel, I. M. 2005, A&A, 436, 47
Efstathiou, A. 1990, Ph.D. Thesis, Univ. London
Efstathiou, A., & Rowan-Robinson, M. 1990, MNRAS, 245, 275
Efstathiou, A., & Rowan-Robinson, M. 1995, MNRAS, 273, 649
Efstathiou, A., Hough, J. H., & Young, S. 1995, MNRAS, 277, 1134
Efstathiou, A., Rowan-Robinson, M., & Siebenmorgen, R. 2000, MNRAS, 313, 734
Farrah, D., Serjeant, S., Efstathiou, A., Rowan-Robinson, M., & Verma, A. 2002, MNRAS, 335, 1163
Farrah, D., Afonso, J., Efstathiou, A., et al. 2003, MNRAS, 343, 585
Galliano, E., Alloin, D., Granato, G. L., & Villar-Martin, M. 2003, A&A, 412, 615
Genzel, R., Lutz, D., Sturm, E., et al. 1998, ApJ, 498, 579
Granato, G. L., & Danese, L. 1994, MNRAS, 268, 235
Granato, G. L., Danese, L., & Franceschini, A. 1997, ApJ, 486, 147
Heisler, C. A., Lumsden, S. L., & Bailey, J. A. 1997, Nature, 385, 700
Hughes, D. H., Serjeant, S., Dunlop, J., et al. 1998, Nature, 394, 241
Kessler, M. F., Steinz, J. A., Anderegg, M. E., et al. 1996, A&A, 315, L27
Krügel, E., & Siebenmorgen, R. 1994, A&A, 282, 407
Kuraszkiewicz, J. K., Wilkes, B. J., Hooper, E. J., et al. 2003, ApJ, 590, 128
Laor, A., & Draine, B. T. 1993, ApJ, 402, 441
Lumsden, S. L., Heisler, C. A., Bailey, J. A., Hough, J. H., & Young, S. 2001, MNRAS, 327, 459
Lumsden, S. L., Alexander, D. M., & Hough, J. H. 2004, MNRAS, 348, 1451
Maiolino, R., Marconi, A., Salvati, M., et al. 2001a, A&A, 365, 28
Maiolino, R., Marconi, A., & Oliva, E. 2001b, A&A, 365, 37
Miller, J. S., & Goodrich, R. W. 1990, ApJ, 355, 456
Morel, T., Efstathiou, A., Serjeant, S., et al. 2001, MNRAS, 327, 1187
Nenkova, M., Ivezic, Z., & Elitzur, M. 2002, ApJ, 570, L9
Okumura, K., ISOCAM PSF Report 1998, http://www.iso.vilspa.esa.es/users/expl_lib/CAM_list.html
Ott, S., et al. 1997, in Astronomical data analysis software and systems VI., ed. G. Hunt, & H. E. Payne, ASP Conf. Ser., 125, 34
Ott, S., Pollock, A., & Siebenmorgen, R. 2000, in ISO Surveys of a Dusty Universe (Springer), ed. D. Lemke, W. Stickel, & K. Wilke, Lect. Notes Phys., 548, 283
Pier, E. A., & Krolik, J. H. 1992, ApJ, 401, 99
Pier, E. A., & Krolik, J. H. 1993, ApJ, 418, 673
Priddey, R. S., & McMahon, R. G. 2001, MNRAS, 324, L17
Rieke, G. H., & Low, F. J. 1975, ApJ, 199, L13
Roche, P. F., Aitken, D. K., Smith, C. H., & Ward, M. J. 1991, MNRAS, 248, 606
Roman, P., & Ott, S. 1999, Report on the behaviour of ISOCAM LW darks, ESA Technical Report, http://www.iso.vilspa.esa.es/users/expl_lib/CAM_list.html
Rowan-Robinson, M. 1992, MNRAS, 258, 787
Rowan-Robinson, M. 1995, MNRAS, 272, 737
Rowan-Robinson, M. 2000, MNRAS, 316, 885
Rowan-Robinson, M., & Crawford, J. 1989, MNRAS, 238, 523
Rowan-Robinson, M., & Efstathiou, A. 1993, MNRAS, 263, 675
Rowan-Robinson, M., Efstathiou, A., Lawrence, A., et al. 1993, MNRAS, 261, 513
Ruiz, M., Efstathiou, A., Alexander, D. M., & Hough, J. 2001, MNRAS, 325, 995
Scott, S. E., Fox, M. J., Dunlop, J. S., et al. 2002, MNRAS, 331, 817
Siebenmorgen, R., Krügel, E., & Laureijs 2001, A&A, 377, 735
Siebenmorgen, R., Krügel, E., & Spoon, H. W. W. 2004a, A&A, 414, 123
Siebenmorgen, R., Freudling, W., Krügel, E., & Haas, M. 2004b, A&A, 421, 129
Silva, L., Granato, G. L., Bressan, A., & Danese, L. 1998, ApJ, 509, 103
Starck, J. L., Siebenmorgen, R., & Gredel, R. 1997, ApJ, 482, 1011
Telesco, C. M., Becklin, E. E., Wynn-Williams, C. G., & Harper, D. A. 1984, ApJ, 282, 427
Tran, H. D. 2001, ApJ, 554, L19
Tran, H. D. 2003, ApJ, 583, 632
van Bemmel, I. M., & Dullemond, C. P. 2003, A&A, 404, 1
Verma, A., Rowan-Robinson, M., McMahon, R., & Efstathiou, A. 2002, MNRAS, 335, 574
Young, S., Hough, J. H., Efstathiou, A., et al. 1996a, MNRAS, 281, 1206
Young, S., Hough, J. H., Efstathiou, A., et al. 1996b, MNRAS, 279, L72